INTERNATIONAL JOURNAL FOR NUMERICAL AND ANALYTICAL METHODS IN GEOMECHANICS
Int. J. Numer. Anal. Meth. Geomech., **23**, 427–438 (1999)

EFFICIENT SOLUTION FOR MATRIX-FRACTURE FLOW WITH MULTIPLE INTERACTING CONTINUA

EDWARD H. SMITH[1]* AND MOHAN S. SETH[2]

[1]*Southern Methodist University, School of Engineering and Applied Science, Dallas, TX 75275, U.S.A.*
[2]*Technical Software & Engineering, Inc., Richardson, TX 75082, U.S.A.*

SUMMARY

An efficient numerical procedure for implementing the multiple interacting continua (MINC) method for fractured porous media in a general-purpose multiphase simulator is presented. This procedure is substantially faster, requires less memory, is amenable to any *n*-component, multiphase non-isothermal package, and is readily adaptable for parallel processing computers. The present procedure results in a reduction of the computing time by a factor of the order of $NMINC^3$ as compared to the band algorithm, where NMINC is the number of nested continua into which each matrix block is further discretized. The memory requirement approaches a reduction factor of the order of $NMINC^2$ for larger problems compared to the band algorithm. The code for the algorithm was structured so as to set up the time consuming, but independent, computations for each matrix block in a subroutine that was parallelized and tested using a Sequent machine accessed under a UNIX environment. For NMINC = 10, total computing time was reduced by 33 per cent for the use of two versus one processor, with the savings increasing for increasing NMINC. The proposed procedure can be implemented with the same ease and efficiency in conjunction with any iterative or direct method, and the grid-blocks can be ordered in any non-standard manner such as in D-4, D-2, and others. Copyright © 1999 John Wiley & Sons, Ltd.

Key words: contaminant transport; fractured porous media; groundwater flow; multiple interacting continua; parallel processing

INTRODUCTION

An accurate simulation of multidimensional multiphase flow in fractured porous media is of considerable interest to environmental engineers and others engaged in the fate and transport of hazardous substances at waste sites.[1] One of the common approaches to describing this type of flow behaviour is by employing the concepts of 'dual porosity', also referred to as Warren and Roots' model.[2] The essence of the model lies in the observations that the fractures have very large permeabilities and, therefore, essentially act as the conduits to fluid flow, while the matrix with much greater volume and storage capacity feeds the fractures associated with it. In order to represent the model in a mathematically tractable form, the fractured porous media was conceptually grouped into two interacting continua with all the fractures in one continuum and

*Correspondence to: Dr. E. Smith, The American University in Cairo, Engineering Department, 113 Sharia Kasr el Aini, PO Box 2511, Cairo 11511, Egypt
†Associate Professor Currently on leave at American University in Cairo, Engineering Department, 113 Sharia Kasr el Aini, PO Box 2511, Cairo 11511 Egypt
‡President

CCC 0363–9061/99/050427–12$17.50

Received 14 October 1997
Revised 24 April 1998

the matrix into another. The flow between the fractures and the matrix is controlled by an interporosity flow parameter which in turn depends on the fracture spacings, orientations, matrix permeability, etc.[2] Pruess and Narasimhan extended the concept of two interacting continua to one with multiple interacting continua (MINC) where the matrix blocks are discretized into a set of nested elements (continua).[3] From thermodynamic equilibrium considerations, they showed that the transient interaction between the matrix and fractures is more realistic and accurate with multiple continua. They also suggested that the MINC approach can be incorporated into any existing simulator which is based on an integral-finite-difference or finite-difference formulation with a relatively modest programming effort.

Zimmerman *et al.*[4] demonstrated that the Warren and Root model with two continua is inadequate for studying transient phenomena, and that the MINC approach should be employed with matrix blocks discretized into ten or more nested continua. They observed, however, that the analysis of large-scale transient problems with the MINC method becomes computationally burdensome and impractical. In order to overcome this deficiency, they initially proposed a semi-analytical treatment for fracture-matrix interflow for single-phase flow, and later extended it to two-phase systems where only one of the phases is mobile. Since their procedure relies on an analytical solution within the matrix, extension of it to a general purpose multiphase flow problem is not obvious.

In the following, an efficient procedure for implementing the MINC method in a general purpose multiphase numerical simulator is presented. This procedure is substantially faster, requires less memory, is easy to implement into an existing code, and is readily adaptable for parallel processing computers. For the purpose of evaluating the procedure, it is implemented here into an existing two-phase, isothermal flow simulator, although the method is amenable to any *n*-component, multiphase non-isothermal package. The computed results are identical to the original formulation by Pruess and Narasimhan,[3] which Zimmerman *et al.*[4] have already demonstrated accurately traces the analytical solution.

MATHEMATICAL MODEL

Flow of liquid and gas phases in the fracture domain is described by the continuity equation incorporating Darcy's law. For the gas phase,

$$\nabla\cdot\frac{Kk_{\mathrm{rg}}}{\mu_{\mathrm{g}}}\rho_{\mathrm{g}}\nabla(p_{\mathrm{g}}-\rho_{\mathrm{g}}gh)+\nabla\cdot G_{\mathrm{d}}K\frac{k_{\mathrm{r}\ell}}{\mu_{\ell}}\rho_{\ell}\nabla(p_{\ell}-\rho_{\ell}gh)+q_{\mathrm{g}}+q_{\ell}G_{\mathrm{d}}+q_{\mathrm{g}f}+q_{\ell f}G_{\mathrm{d}}$$
$$=\frac{\partial}{\partial t}\phi(\rho_{\mathrm{g}}S_{\mathrm{g}}+\rho_{\ell}S_{\ell}G_{\mathrm{d}}) \tag{1}$$

For the liquid phase,

$$\nabla\cdot\frac{Kk_{\mathrm{r}\ell}}{\mu_{\ell}}\rho_{\ell}\nabla(p_{\ell}-\rho_{\ell}gh)+q_{\ell}+q_{\ell f}=\frac{\partial}{\partial t}(\phi\rho_{\ell}S_{\ell}) \tag{2}$$

The flow equations in the matrix are analogous to the above except that the flow is restricted in one dimension with no gravity, as per MINC formulation, and may be written as

$$\frac{\partial}{\partial x}\left(K\frac{k_{\mathrm{rg}}}{\mu_{\ell}}\rho_{\mathrm{g}}\right)_{\mathrm{m}}\left(\frac{\partial p_{\mathrm{gm}}}{\partial x}\right)_{\mathrm{m}}+\frac{\partial}{\partial x}G_{\mathrm{d}}\left(K\frac{k_{\mathrm{rl}}}{\mu_{\ell}}\rho_{\mathrm{l}}\right)_{\mathrm{m}}\frac{\partial p_{\ell\mathrm{m}}}{\partial x}-q_{\mathrm{g}f}=\frac{\partial}{\partial t}\phi_{\mathrm{m}}(\rho_{\mathrm{g}}S_{\mathrm{g}}+\rho_{\ell}S_{\ell}G_{\mathrm{d}})_{\mathrm{m}} \tag{3}$$

$$\frac{\partial}{\partial x}\left(K\frac{k_{r\ell}}{\mu_\ell}\rho_\ell\right)_m\frac{\partial p_{\ell m}}{\partial x}-q_{\ell f}=\frac{\partial}{\partial t}\phi_m(\rho_\ell S_\ell)_m \tag{4}$$

where subscripts ℓ and g represent liquid and gas phase, respectively, and m refers to the matrix. Other parameters and variables are pressure (p), saturation (S), density (ρ), gravitational acceleration vector (g), depth (positive downward, h), source/sink (q), absolute rock permeability (K), relative permeability (k_r), porosity (ϕ), dissolved gas in liquid phase (G_d), viscosity (μ), spatial dimension for the matrix (x), and time (t). The terms $q_{\ell f}$ and q_{gf} represent flow between the matrix and fractures through the interface between them. The *del* operator for cartesian and cylindrical geometry, respectively, is:

$$\nabla\cdot F=\frac{\partial F_x}{\partial x}+\frac{\partial F_y}{\partial y}+\frac{\partial F_z}{\partial z}\quad\text{(cartesian)}$$

$$\nabla\cdot F=\frac{1}{r}\frac{\partial}{\partial r}(F_r r)+\frac{1}{r}\frac{\partial F_\theta}{\partial\theta}+\frac{\partial F_z}{\partial z}\quad\text{(cylindrical)}$$

Additional auxiliary relations are

$$S_\ell+S_g=1 \tag{5}$$

$$p_g-p_\ell=p_{cl,f} \tag{6}$$

$$S_{\ell m}+S_{gm}=1 \tag{7}$$

$$p_{gm}-p_{\ell m}=p_{cl,m} \tag{8}$$

where p_{cl} is the gas–liquid capillary pressure.

Equation (1)–(8) can be solved using appropriate boundary conditions for the eight unknowns, namely: p_ℓ, p_g, $p_{\ell m}$, p_{gm}, S_ℓ, S_g, $S_{\ell m}$ and s_{gm}. The initial and boundary conditions considered are:

$p=p(x,y,z,t=0)$ an arbitrary initial pressure field in the fractures

$S_\ell=S_\ell(x,y,z,t=0)$ an arbitrary initial saturation field in the fractures

$p_m=p_m(x,y,z,t=0)$ an arbitrary initial pressure field in the matrix

$S_{\ell m}=S_{lm}(x,y,z,t=0)$ an arbitrary initial saturation field in the matrix

and no flow at the boundary, given by

$$\frac{\partial(p_\ell-\rho_\ell gh)}{\partial\hat{n}}=\frac{\partial(p_g-\rho_g gh)}{\partial\hat{n}}=0 \tag{9}$$

$$q_{\ell f}=T(p_\ell-p_{\ell m})\frac{k_{r\ell}}{\mu_\ell}\rho_\ell$$

$$q_{gf}=T(p_g-p_{gm})\frac{k_{rg}}{\mu_g}\rho_g+q_{\ell f}G_d \tag{10}$$

where $\hat{n}$ is a unit vector normal to the system boundary, and T is the matrix-fracture interfacial transmissibility.

These equations are highly non-linear and, therefore, must be solved numerically. An implicit finite-difference procedure was employed as outlined below.

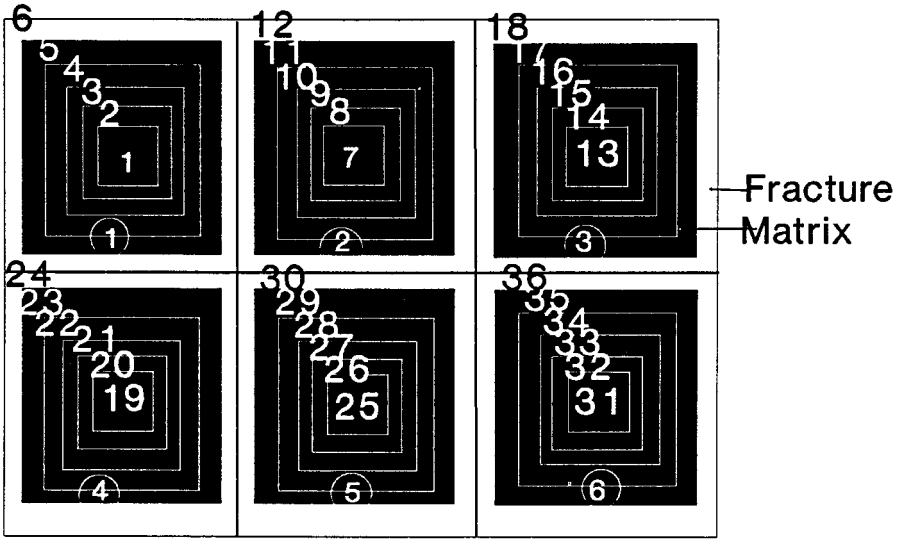

Figure 1. Conceptual MINC structure for a two-dimensional (xy) system. Circled numbers refer to matrix-fracture blocks. Number of MINC elements in each block (NMINC) equals 6. Adapted from Pruess and Narasimhan (1985).

FINITE-DIFFERENCE ANALOGUE

Consider a fracture-matrix domain discretized into NX, NY, and NZ blocks in x, y, and z coordinate directions, respectively. Let NMINC be the number of nested continua into which each block is further subdivided. The outermost continuum represents the fracture, and the remaining (NMINC-1 interior members) belong to the matrix (Figure 1).

Writing the space derivatives in five-point central difference and the time derivatives in backward finite-difference forms, we obtain the following implicit representations for flow in the fracture and matrix:

$$\Delta(T_{\mathrm{g}} + T_{\ell} G_{\mathrm{d}})^{n+1} \Delta(p_{\mathrm{g}} - \rho_{\mathrm{g}} g h)^{n+1} + (q_{\mathrm{g}} + q_{\ell} G_{\mathrm{d}})^{n+1} + (q_{\mathrm{gf}} + q_{\ell \mathrm{f}} G_{\mathrm{d}})^{n+1}$$

$$= \frac{V_{\mathrm{B}}}{\Delta t} \delta [\rho_{\mathrm{g}}(1 - S_{\ell}) + \rho_{\ell} S_{\ell} G_{\mathrm{d}}] \phi \tag{11}$$

$$\Delta T_{\ell}^{n+1} \Delta(p_{\mathrm{g}} - p_{\mathrm{cl}} - \rho_{\ell} g h)^{n+1} + q_{\ell}^{n+1} + q_{\mathrm{lf}}^{n+1} = \frac{V_{\mathrm{B}}}{\Delta t} \delta \rho_{\ell} S_{\ell} \phi \tag{12}$$

$$\Delta(T_{\mathrm{g}} + T_{\ell} G_{\mathrm{d}})_{\mathrm{m}}^{n+1} \Delta p_{g,m}^{n+1} - q_{\mathrm{g,f,m}}^{n+1} = \frac{V_{\mathrm{B},m}}{\Delta t} \delta [\rho_{\mathrm{g}}(1 - S_{\ell}) + \rho_{\ell} S_{\ell} G_{\mathrm{d}} \phi]_{\mathrm{m}} \tag{13}$$

$$\Delta T_{\ell \mathrm{m}}^{n+1} \Delta(p_{\mathrm{g}} - p_{\mathrm{cl}})_{\mathrm{m}}^{n+1} - q_{\ell,\mathrm{f,m}}^{n+1} = \frac{V_{\mathrm{B,m}}}{\Delta t} \delta(\rho_{\ell} S_{\ell} \phi)_{\mathrm{m}} \tag{14}$$

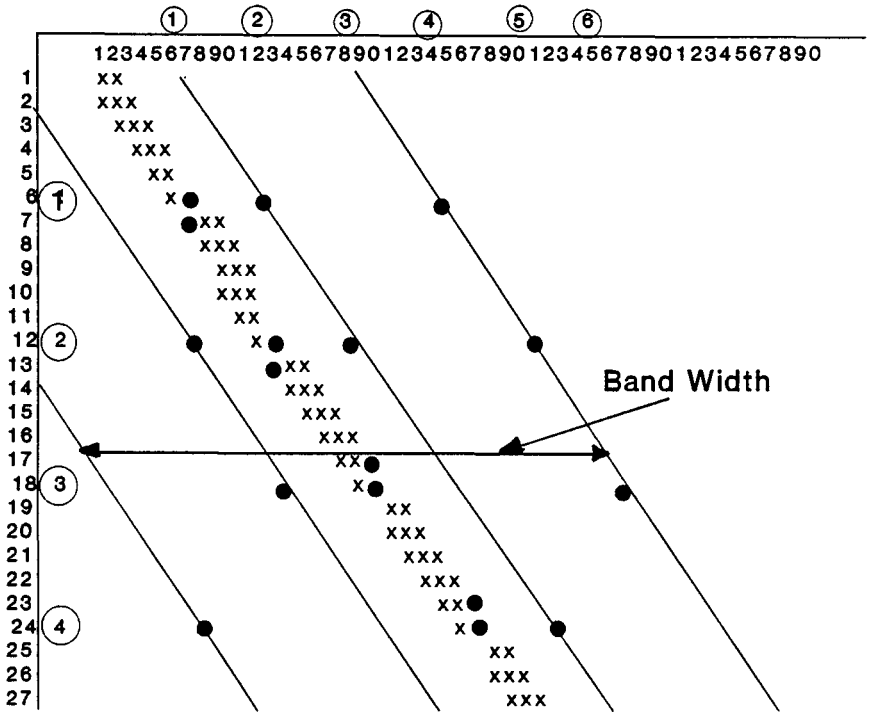

Figure 2. Matrix structure for MINC formulation corresponding to Figure 1

where the operator

$$\Delta T\,\Delta\Phi = T_{i+1/2,j,k}(\Phi_{i+1,j,k} - \Phi_{i,j,k}) + T_{i-1/2,j,k}(\Phi_{i-1,j,k} - \Phi_{i,j,k}) + T_{i,j+1/2,k}(\Phi_{i,j+1,j,k} - \Phi_{i,j,k}) + T_{i,j-1/2,k}(\Phi_{i,j-1,k} - \Phi_{i,j,k}) + T_{i,j,k+1/2}(\Phi_{i,j,k+1} - \Phi_{i,j,k}) + T_{i,j,k-1/2}(\Phi_{i,j,k-1} - \Phi_{i,j,k})$$

For matrix flow, the operator applies only in the i-direction. In addition,

$$\delta X = X^{n+1} - X^n$$

where the superscripts n and $n+1$ refer to the time level; the block volume $V_B = \Delta x \Delta y \Delta z$; the time step size $\Delta t = t^{n+1} - t^n = \delta t$; and phase transmissibility in the i-direction is

$$T_{a,i+1/2,j,k} = \left(\frac{Kk_{ra}}{\mu_a}\rho_a\right)_{i+1/2}\left(\frac{\Delta y \Delta z}{\Delta x}\right)_i$$

Similar terms for the transmissibility are written for the j and k directions. The subscript a may refer to either ℓ or g. In the above expressions, the liquid-phase pressure and gas-phase saturations have been eliminated by substitution of the auxiliary relationships. Furthermore, the transmissibilities are evaluated at the block interfaces such that the absolute permeability is

estimated as the harmonic average,[5] the relative permeability is assumed to be the upstream value, and the density and viscosity are calculated as arithmetic averages.

Equations (11)–(14) represent a set of $2 \times \mathrm{NB} \times \mathrm{NMINC}$ non-linear algebraic equations of the form: $R_e(p_g, p_{gm}, S_\ell, S_{\ell m})^{n+1} = 0$, where $e = 1, 2, 3, 4$ corresponds to finite-difference equations (11)–(14), and NB is the number of blocks within the fracture domain. To handle the non-linearities, the equations are linearized using a Newton–Raphson iteration procedure of the form

$$R_e^{k+1} = R_e^k + \sum \frac{\partial R_e}{\partial X_e} \delta X_e \quad (X_e = p_g, p_{gm}, S_\ell, S_{\ell m}) \tag{15}$$

The iteration cycle is continued until the residual error is within the specified tolerance. The coefficient matrix arising from equations (15) is shown in Figure 2. The solid dots represent the coefficients for the fracture domain, while the x's represent the coefficients for the matrix elements. The standard ordering of the blocks lead to a banded matrix of bandwidth $(2 \times \mathrm{NZ} \times \mathrm{NY} \times \mathrm{NMINC} + 1) \times \mathrm{np}$ ($\mathrm{np} = 2$ for the current example of two components), with a total of $\mathrm{NX} \times \mathrm{NY} \times \mathrm{NZ} \times \mathrm{NMINC} \times \mathrm{np} = \mathrm{NB} \times \mathrm{NMINC} \times \mathrm{np}$ equations, where $\mathrm{NB} = \mathrm{NX} \times \mathrm{NY} \times \mathrm{NZ}$ = total number of fracture blocks.

DECOMPOSITION OF FRACTURE-MATRIX EQUATIONS

The computational efficiency realized in the above formulation results primarily from decoupling the fracture and matrix equations rather than solving them simultaneously. It should be emphasized that the decoupling procedure maintains a full degree of implicitness that is, in fact, identical to that of the simultaneous solution.

A careful examination of the basic governing equations reveals that only the interfracture-matrix flow term, q_{pf}, couples the two domains, otherwise they are completely uncoupled. This is reflected in the coefficient matrix in that only the outermost element of the matrix is coupled to the associated fracture block. Furthermore, the coefficients corresponding to the rock matrix have the structure of a typical one-dimensional (1-D) problem corresponding to a tridiagonal matrix. Therefore, the rock matrix equations can be solved independently of each other in terms of the fracture pressure and saturations employing the simple Thomas algorithm for 1-D problems. By this approach, the last equation during the forward sweep of the tridiagonal matrix solution takes the form

$$C_m \delta X_m = R_m - C_f \delta X_f \tag{16}$$

where C, δX, and R are, respectively, the coefficients, change in the solution vector over a time step, and the residual; and the subscript 'm' refers to the outermost matrix element (i.e. NMINC-1), and 'f' refers to the fracture. Substitution for δX_m from equation (16) into the fracture equation eliminates any coupling between the fracture and the matrix, and we are now able to solve the modified equations for the fractured domain independent of the matrix equations. Once the reduced set of equations corresponding to the fractures is solved for δX_f, we use equation (16) to obtain the solution of δX_m for the outermost element of the matrix and complete the backward sweep for the rest of the matrix elements. Note that in this procedure, the fractured domain equations can be solved by any iterative (including sparse matrix) or direct method.

COMPUTATIONAL AND MEMORY REQUIREMENTS

The work required in terms of multiplications and divisions for a matrix with MINC formulation using the band algorithm for a single phase problem with large NX, NY or NZ is approximately;

$$W_{\text{band}} = \text{NB} \times \text{NMINC} \times (\text{NY} \times \text{NZ} \times \text{NMINC})^2 \tag{17}$$

Note that $\text{NY} \times \text{NZ} \times \text{NMINC}$ is half of the band-width of the matrix. The new formulation solves, NB times, the 1-D problem of dimensions NMINC-1, and the fracture problem of NB grid blocks. The work required for a 1-D problem is $5 \times (\text{NMINC-1})\text{-}4$. Therefore, the total work estimate with the present formulation is

$$W_{\text{new}} = \text{NB} \times [5 \times \text{NMINC} - 1) - 4] + \text{NB} \times (\text{NY} \times \text{NZ})^2 \tag{18}$$

Thus, the work ratio of the band and the new method is

$$\frac{W_{\text{band}}}{W_{\text{new}}} = \frac{\text{NMINC} \times (\text{NY} \times \text{NZ} \times \text{NMINC})^2}{(\text{NY} \times \text{NZ})^2 + 5 \times \text{NMINC} - 9} \tag{19}$$

if $(\text{NY} \times \text{NZ})^2 \gg 5 \times \text{NMINC-9}$, the work ratio from equation (19) approaches NMINC^3. Thus, for a typical problem with NMINC of 8–10 elements, the theoretical work ratio would range from 512 to 1000. We can perform a similar exercise for 2 or more unknowns per grid-block by simply multiplying the bandwidth and the number of equations by np (the number of phases or unknowns per element).

Storage required by the band algorithm is

$$M_{\text{band}} = [\text{NB} \times \text{NMINC} \times (2 \times \text{NY} \times \text{NZ} \times \text{NMINC} + 1)] \times \text{np} \times \text{np} \tag{20}$$

For the new algorithm:

$$M_{\text{new}} = [\text{NB} \times (2 \times \text{NY} \times \text{NZ} + 1) + \text{NB} \times (2 \times \text{NMINC} + 1)] \times \text{np} \times \text{np} \tag{21}$$

The ratio of M_{band} to M_{new} is

$$\frac{M_{\text{band}}}{M_{\text{new}}} = \frac{\text{NMINC} \times (2 \times \text{NY} \times \text{NZ} \times \text{NMINC} + 1)}{2 \times (\text{NY} \times \text{NZ} + 1 + \text{NMINC})} \tag{22}$$

Thus, for a 2-D problem with $\text{NMINC} = 10$, $\text{NY} = 20$, and $\text{NZ} = 1$, the storage ratio is $= 64{\cdot}6$. In general, for large 3-D problems (when $\text{NY} \times \text{NZ} \gg \text{NMINC} + 1$), the ratio approaches a factor of NMINC^2.

PARALLELIZATION

Implicit finite-difference techniques have been shown to be adaptable for taking advantage of highly coupled, shared memory, parallel architectures.[6] Due to the topology of the matrix decomposition formulated here, the new algorithm is ideally suited for parallel computation. To demonstrate this and the potential reduction in computation time achievable through a parallel implementation, an algorithm (in FORTRAN) was developed and tested on a Sequent machine accessed under a UNIX environment.[7] The Sequent Symmetry system used in this exercise has 20 Intel 386 processors, up to nineteen of which are accessible for a single application, and a tightly coupled, MIMD, shared memory. In our coding logic, the accumulation and flux terms and their derivatives were computed by the same subroutines for both the matrix and fracture equations.

Thus, no additional efforts were required in setting up the Jacobian for the matrix equations. A driver subroutine for decoupling the fracture and matrix flow sets up the Jacobian for 1-D matrix flow through calls to the common routines, and then calls the 1-D solver. Since the flow within each of the NM matrix blocks is independent of other blocks (except for the coupling at the matrix–fracture interface discussed above), only this routine was parallelized to investigate the effectiveness of parallelization.

Alternatively, the algorithm may be readily implemented on a set of UNIX workstations using Parallel Virtual Machine (PVM) software.[8] PVM enables a collection of heterogeneous computers to be used as a coherent and flexible concurrent computational resource. It provides the programmer with process control and communication routines to link tasks running on different host machines. In the implementations of the above procedure with PVM, the master-slave model may be used. Key considerations for any efficient virtual machine parallelization are that network speed must be high and the data transfer across the network should be minimal. It is fortunate that the amount of data transfer in this case involves only the coefficients at the matrix–fracture interface.

DISCUSSION

The computational performance with respect to the band algorithm is presented here primarily because it is computationally robust and widely used, although variations of D2 and D4 ordered Gauss elimination procedures are generally superior.[9] Table I shows the computing time in seconds for two small problems with a varying number of MINC elements and np equal to 2. These runs were carried out on a PC-486/66. Comparative runs with a large number of blocks were not practical due to the machine limitations. All runs were made with an implicit two-phase isothermal simulator assuming two unknowns per element. The new algorithm was used in conjunction with a D4 ordered Gaussian elimination for the fracture equations.

For the 7×7 matrix runs, the ratio of CPU time per time step for the band versus the proposed algorithm is about four to five times the work ratio predicted by Equation (19). The ratio increases to about ten times that predicted from equation (19) when the problem is expanded to 10×10. The ratio of K-words of memory for calculations by the band versus proposed algorithm is approximately one half of the storage requirement ratio estimated according to equation (22), and changed little for increase in the matrix size from 7×7 to 10×10.

A large set of equations, as in MINC formulation, limits the applicability of the band algorithm due to round-off errors and the excessive computing requirements. Iterative methods are preferable for large problems, but fully implicit treatment and large transmissibility associated with fractures may render the matrix arising from such systems weakly or even non-diagonally dominant. This in turn results in convergence difficulties and requires excessively small time steps. It is important to note that even when an iterative method is applicable, the decomposition procedure presented above is more efficient and can be used advantageously in solving the fracture domain equations using said method. This is because about 90 per cent of the blocks (assuming 10 interacting continua) are suitable for one-dimensional treatment; only the fracture elements require solution by an iterative method. The decomposition procedure, therefore, enables use of an efficient solver (such as the Thomas algorithm for these 90 per cent of the blocks.

Several numerical experiments with a sparse matrix technique, MA28 algorithm,[10] illustrate the point. Using the proposed matrix decomposition procedure together with a sparse matrix solver for the fracture continuum, a 40-fold reduction in cpu time (per iteration) and 10-fold

Table I. Comparison of band versus proposed algorithm

Problem size	No. of MINC elements (NMINC)	CPU time per time step		Memory (K-words)	
		Band algorithm	Proposed algorithm	Band algorithm	Proposed algorithm
7×7	5	24·32	0·040	112·00	8·22
7×7	7	73·23	0·050	218·99	9·48
7×7	10	296·85	0·070	445·56	11·37
10×10	5	118·01	0·075	202·00	12·80
10×10	7	334·50	0·084	394·80	14·40
10×10	10	988·90	0·100	804·00	16·80

Table II. Parallelization statistics for 10×15 matrix using sequent machine

NMINC	Number of processors	Total computing time (s)	Time in parallelized subroutine (s)	% Utilization of multiple processors
7	1	80·0 (79·2)	49·5 (49·5)	—
	2	54·9 (55·0)	25·3 (25·4)	97·8 (97·4)
	3	46·9 (46·9)	17·3 (17·3)	95·4 (95·4)
	5	40·4 (40·4)	10·9 (10·8)	90·8 (91·7)
	10	37·4 (36·0)	6·67 (6·36)	74·2 (77·8)
	15	34·5 (34·3)	4·65 (4·61)	71·0 (71·6)
10	1	94·0	62·8	—
	2	63·4	32·2	97·5
	3	53·2	21·8	96·0
	5	45·1	13·7	91·7
	10	38·9	7·6	82·6
	15	36·9	5·76	72·7
15	1	118·1	84·5	—
	2	76·8	43·0	98·3
	3	63·1	29·5	95·5
	5	51·8	18·1	93·3
	10	45·6	10·6	79·7
	15	40·5	6·99	80·6
20	1	141·9	106·1	—
	2	90·4	54·4	97·5
	3	72·7	36·7	96·4
	5	58·6	22·7	93·5
	10	52·0	13·7	77·4
	15	44·8	8·79	80·5

reduction in memory requirement were achieved over the MA28 algorithm for a two-dimensional problem (7×7 with 10 MINC elements). The cpu ratio decreases somewhat with increasing size of the matrix or for expansion to a three-dimensional problem, but increases with the number of MINC elements. An additional advantage of the proposed decomposition method is that up to a certain number of fracture blocks, a direct solver could still be competitive and robust, which

would not be the case if the matrix is not decomposed and the full set of equations are solved by a direct method.

Potential gains in computational efficiency that can be achieved through parallelization are illustrated in Table II for a 10×15 test matrix using the Sequent Symmetry machine. Viability of parallelization for this application is evident from the fraction of computing time required for solving the block equations, which is accomplished in the parallelized subroutine. For NMINC = 7, more than 60 per cent of the total computing time is consumed in the parallelized routine, and this percentage increases with the number of MINC elements (e.g. 75 per cent for NMINC = 20). Therefore, gains in gross computation time also increase with NMINC. Numbers in parentheses in Table II represent values for independent simulations as an illustration of the precision of the experiment.

The effectiveness and optimization of multiple processors for a given application can be assessed by calculating the percent utilization, U:

$$U = \left(\frac{T_1}{T_N \cdot N}\right) \times 100\% \tag{23}$$

where T_1 is the computing time consumed in the parallelized routine when one processor is used, and T_N is the time used by multiple processors, N. As anticipated, U decreases for an increasing number of processors as a result of increasing overhead time associated with transfer of information between individual processors and the system bus.

CONCLUSIONS

1. The present procedure results in a reduction of the computing time by a factor of the order of NMINC^3 as compared to the band algorithm. The computational efficiency is also superior to any iterative method.
2. The memory requirement is substantially reduced, and approaches a reduction factor of the order of NMINC^2 for large problems using band algorithm.
3. The new algorithm readily lends itself for parallel architecture computers and PVM; this work has demonstrated improved computational efficiency on the former.
4. The procedure can be implemented with the same ease and efficiency in conjunction with any iterative or direct method, and the grid-blocks can be ordered in any non-standard manner such as in D-4, D-2, and others.
5. It is readily applicable for single and multiphase multicomponent isothermal and non-isothermal problems.

APPENDIX

Notation

C	coefficients for elements in tridiagonal solution matrix
g	gravitational acceleration, $L \cdot t^{-2}$
G_d	dissolved gas in liquid phase
h	vertical depth (positive downward), L

k_r	relative permeability
K	absolute rock permeability, L^2
M	memory requirement
$\hat{n}$	unit vector normal to boundary
N	number of processors in parallel computations
NB	number of blocks in fracture domain
NMINC	number of nested continua for each matrix block
NX	number of divisions in x-direction of domain of length Δx
NY	number of divisions in y-direction of domain of length Δy
NZ	number of divisions in z-direction of domain of length Δz
p	pressure, $M \cdot L^{-1} \cdot t^{-2}$
p_{cl}	gas–liquid capillary pressure, $M \cdot L^{-1} \cdot t^{-2}$
q_{gf}	interfacial gas flow between matrix and fracture, $L^3 \cdot t^{-1}$
$q_{\ell f}$	interfacial liquid flow between matrix and fracture, $L^3 \cdot t^{-1}$
r	radial distance for cylindrical co-ordinates, L
R	computational residual
S	saturation
t	time
T	matrix-fracture interfacial transmissibility
T_1	parallel computing time using one processor, t
T_N	parallel computing time using N processor, t
U	per cent utilization of multiple processors
V_B	finite-difference block volume, L^3
W	computational work requirement (no. multiplications and divisions)
x, y, z	space directions for domain, L
$\mathbf{X}$	solution vector of unknown pressures and saturations
θ	angle for cylindrical coordinates, deg
μ	dynamic viscosity, $M \cdot L^{-1} \cdot t^{-1}$
ϕ	porosity
ρ	density, $M \cdot L^3$

Superscripts

n	time level of numerical calculations

Subscripts

a	variable (may be l or g)
band	band algorithm
e	variable for equation no. designation
f	fractures
g	gas phase
i, j, k	directional designation
ℓ	liquid
m	matrix
new	modified solution algorithm

REFERENCES

1. R. Therrien and E. A. Sudicky, 'Three-dimensional analysis of variably-saturated flow and solute transport in discretely-fractured porous media, *J. Contam. Hydrol.*, **23,** 1–44 (1996).
2. J. E. Warren and P. J. Root, 'The behavior of naturally fractured reservoirs', *Soc. Pet. Engng. J.*, **3,** 245–255 (1963).
3. K. Pruess and T. N. Narasimhan, 'A practical method for modeling fluid and heat flow in fractured porous media', *Soc. Pet. Engng. J.*, **25,** 14–26 (1985).
4. R. W. Zimmerman, G. Chen, T. Hadgu and G. S. Bodvarsson, 'A numerical dual-porosity model with semianalytical treatment of fracture/matrix flow', *Wat. Resour. Res.*, **29,** 2127–21367 (1993).
5. H. S. Carslaw and J. C. Jaeger, *Heat Conduction in Solids*, Clarendon Press, Oxford, UK, 1959.
6. A. N. Varghese and P. E. Raad, 'Synchronization-free parallel implementation of factored-implicit and explicit techniques', *Comp. Fluid Dyn.*, **6,** 137–155 (1996).
7. Sequent Computer Systems, *Guide to parallel programming*, 3rd edn., Prentice-Hall, Englewood Cliffs, NJ, 1992.
8. A. Beguelin, J. Dongarra, A. Geist and V. Sunderam, 'Visualization and debugging in a heterogeneous environment', *Computer*, **26,** 88–95 (1993).
9. H. S. Price and K. H. Coats, 'Direct methods in reservoir simulation', *SPE #4278, Presented at the 3rd SPE Symp. on Numerical Simulation*, Soc. of Pet. Eng. of AIME, Houston, TX, 1973.
10. I.S. Duff, 'MA28—a set of FORTRAN subroutines for sparse unsymmetrical linear equations', *AERE Harwell Report R* 8730, 1977.

